CHAPTER 2

FINITE ELEMENT METHODS FOR ANALYZING A BAND GAP CHARACTERISTIC OF TWO DIMENSIONAL PHOTONIC CRYSTALS

This chapter provides basic knowledge of finite element method (FEM) for analyzing the band gap characteristic of 2D PCs. The formulation and programming procedures of the FEM will be explained in this chapter. The FEM formulation with linear triangular elements and polygonal elements based on Wachspress interpolation, are investigated in this thesis. In this chapter, the FEM formulation based on linear triangular element will be explained, while the FEM formulation based on polygonal element will be explained in the next chapter.

2.1 Definition of The Problems

2.1.1 Physical Structures of Two Dimensional Photonic Crystals

In telecommunication and some other fields nowadays, the invention of new materials and devices keeps going on. One of the major contributions is due to the invention of photonic crystals by Yablonovitch and John in 1987 [1]. Photonic crystals are artificially periodic structures that can be one-, two- or three-dimension in nano-scale length where the periodicity is in light wavelength-scale. The in-line light propagation that passes the periodicity will experience a photonic band gap (PBG). A PBG material exhibits a forbidden frequency band where no available mode can propagate or exist inside the band gap. We can take advantage from the band gap phenomena to unlock the enormous potential in utilizing PBG materials for developing new integrated optical devices. The integrated optical devices play an important roles in high-speed optical communication networks, particularly in the production of purely optical circuits for dense wavelength-division multiplexing [23].

The examples of structures of a 2D PC with square and triangular lattice constants can be shown in Figure 2.1. The periodicity of the structure are obtained by positioning rods or holes in a periodic arrangements such as a square lattice constant or a triangular lattice constant in a two dimensional space. Both lattice constants presented in the figure are the most famous ones among the other types of lattice constant. The design of square lattice PC are the most simple and easy to analyze so that they are very appropriate to be utilized as a model structure in order to test a new method or to investigate their characteristics. This work employs them as a test patch for the FEM in the preliminary research. The other type is the triangular lattice PC. This type of lattice is proved to be able to provide a complete band gap where the gap can exist and overlap in both TM and TE modes. It is extensively used because it can make the optical wave confined to be guided [5].
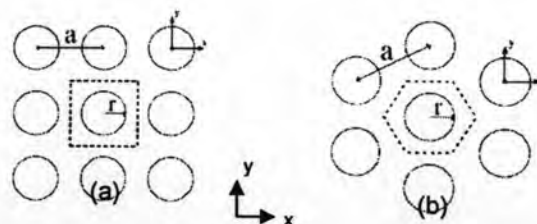
Figure 2.1 (a) Square and (b) triangular lattice constant [7].

2.1.2 Defining the Unit Cell of Two Dimensional Photonic Crystals

The FEM must be applied to a specific calculation domain that is defined previously in which the solutions are taken. In general problem, the calculation domain can be attained from the whole domain of the structure or some parts of the real structure as a point of interest such as a resonator or a waveguide. In case where the structure has a periodic geometry, the electromagnetic field solutions of light in the structure will be periodic as well. This knowledge allows us to regard only one periodic area of the whole region of the domain as domain for computation. One sample of periodic areas is called a unit cell utilized as a calculation domain in FEM.

To determine the unit cell in 2D PCs is quite simple by applying the Weigner Seitz cell algorithm [10]. The algorithm can be listed as follows:

1. From the periodic arrangement in the structure, choose the center point of interest as the given lattice point.
2. Draw the lines to connect the given lattice point to all nearby lattice points.
3. At the mid-points and normal to these lines, draw new lines so that these line can be intersection to another line.
4. The intersections will yield a smallest area called the Weigner-Seitz primitive cell, which is known as a first Brillouin zone and is considered as the unit cell.

Figure 2.2 shows the illustration of this algorithm where the square shaded region represents the first Brillouin zone (BZ) and the shadowed triangular region is the irreducible Brillouin zone in reciprocal lattice. This last mentioned zone is the smallest zone in the BZ where it can repeat to other region inside the first BZ properly under symmetry translations and rotations. This zone is used to define the wave vectors such that it can be called a wave vector zone. Examples of both square and triangular unit cells are shown in Figure 2.1. The physical structure of 2D PCs is described in terms of a lattice as well as the crystal structure where the holes or the rods are placed in the lattice points as shown in Figure 2.2a for square lattice PCs and Figure 2.2b for triangular lattice ones. In such a unit cell, there is always one lattice point.
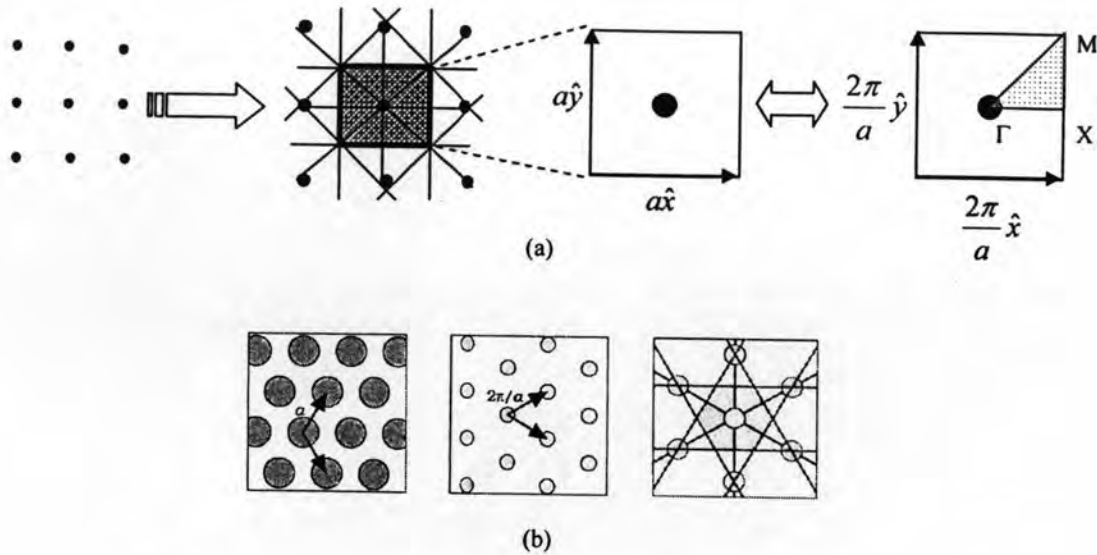
Figure 2.2 Construction of a Weigner-Seitz cell on (a) a square and (b) a triangular
lattice constant PCs (Joannopoulos, 1995) in a x-y plane.

The lattice is defined by the three translation vectors $\vec{a}_1, \vec{a}_2$, and $\vec{a}_3$ [10] in such a
way that the repetition distance can be maintained. Since the problem consider only with
two dimensional vectors, there translational vectors can be expressed as a combination of
2 base vector $\vec{a}_1$ and $\vec{a}_2$. Thus, translation vector can be defined as follows:

$$\vec{T} = u_1 \vec{a}_1 + u_2 \vec{a}_2 \tag{2.1}$$

where u_1 and u_2 are integers. This is also called as a primitive lattice vector where it says
that there is no other smaller regions that can represent the unit cell of the structure so that
the cell is also presented as a primitive cell. This primitive cell can fill all the surface of
the structure by repetition of a proper translation.

Another type of lattice in crystal structure is a reciprocal lattice, where reciprocal
lattice vector can be represented in vector form as follows.

$$\vec{G} = v_1 \vec{b}_1 + v_2 \vec{b}_2 \tag{2.2}$$

where $\vec{b}_1$ and $\vec{b}_2$ are the primitive vectors of the reciprocal lattice while v_1 and v_2 are
integers. The vector $\vec{G}$ represents the reciprocal lattice vector. A diffraction pattern of
such crystal is a map of reciprocal lattice of the crystal while the image of the crystal is a
map of the crystal structure in real space. The relation between these two lattices in two-
dimensional spaces is given by the definition as follows.

$$\vec{b}_1 = {2\pi}/{\vec{a}_1} \tag{2.3}$$

$$\vec{b}_2 = {2\pi}/{\vec{a}_2} \tag{2.4}$$

with a property of $\vec{b}_i \cdot \vec{a}_j = 2\pi\delta_{ij}$.

Vectors in the direct lattice have the dimension of [length] in meter (m), while the vectors in reciprocal lattice have the dimension of [1/length] and the unit becomes m^{-1} or if we express in term of 2π then the unit will be rad.m^{-1}. The reciprocal lattice is a lattice in the Fourier space associated with the crystal. Since the wave vectors are always presented in Fourier space, every position in Fourier space may have a meaning as a description of a wave. However, there is a special significance to the points defined by the set of $\vec{G}$'s associated with a crystal structure.

The Fourier series is presented as follows,

$$n(\vec{r}) = \sum_{\vec{G}} n_{\vec{G}} \exp(i\vec{G} \cdot \vec{r}) \tag{2.5}$$

where $n(\vec{r})$ is a periodic function, $n_{\vec{G}}$ is a Fourier coefficient, $\vec{r}$ is a vector position, and finally $\vec{G}$ here is the reciprocal lattice vector. When there is a translation of the point position in the crystal such as in (2.1), the Fourier series becomes

$$n(\vec{r} + \vec{T}) = \sum_{\vec{G}} n_{\vec{G}} \exp(i\vec{G} \cdot \vec{r}) \exp(i\vec{G} \cdot \vec{T}) \tag{2.6}$$

where

$$\begin{aligned}\exp(i\vec{G} \cdot \vec{T}) &= \exp\left[i\left(v_1\vec{b}_1 + v_2\vec{b}_2\right) \cdot \left(u_1\vec{a}_1 + u_2\vec{a}_2\right)\right] \\ &= \exp\left[i2\pi\left(v_1u_1 + v_2u_2\right)\right] \\ &= 1\end{aligned}$$

Thus, $n(\vec{r} + \vec{T}) = n(\vec{r})$. $\qquad\qquad(2.7)$

This shows that the periodic function is achieved in terms of the Fourier series when the reciprocal lattice vector $\vec{G}$ is included [10].

2.1.3 Defining the Wave Vectors of Two Dimensional Photonic Crystals

The wave vectors employed in calculating the band gap characteristic are very important because they are used as the input values in order to get the solutions of eigensystem. For each defined wave vector, the solution is a set of eigenfrequencies with related eigenfunctions of fields. These wave vectors are defined from the irreducible Brillouin zone within Γ-X-M-Γ area for a square unit cell and in Γ-M-K-Γ area for hexagonal unit cell shown in Figure 2.3. The defined area of the zone inside the BZ can be positioned anywhere under a translational symmetry and a rotational symmetry. Based on the construction, the edges of this irreducible BZ show the main directions where the periodicities is on the unit cell. The parent zone of it, i.e. the BZ, is defined as a Weigner-seitz primitive cell in the reciprocal lattice.

To define the wave vectors in 2D PCs, the problem will be reduced into one dimensional PCs (1D PCs) in order to investigate the concept and the relation among the

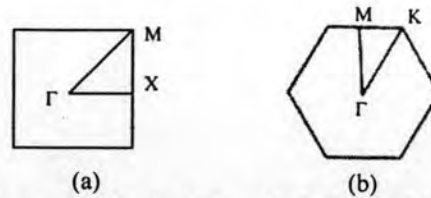wave vectors, the direct lattice vector, and the reciprocal lattice vector. Figure 2.4 shows an example of 1D PCs.

(a)   (b)

Figure 2.3 A unit cell (the first BZ) with the irreducible BZ in (a) square and (b) triangular lattice constants.

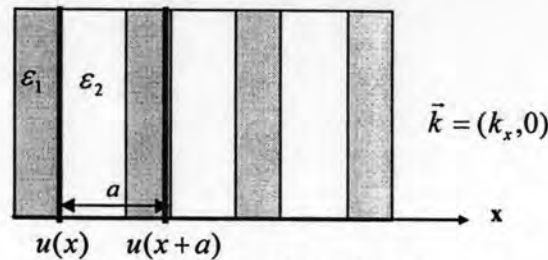

$\vec{k} = (k_x, 0)$

$u(x)$ $u(x+a)$

Figure 2.4 A model of a 1D PC

Taking the concept of Fourier series in reciprocal lattice in (2.5)-(2.7) and bringing them into one dimensional problem, the equation in (2.5) for one periodicity can be changed into:

$$n(x\vec{a}_1) = n_G \exp(i(v_1\vec{b}_1)\cdot(x\vec{a}_1)) \tag{2.8}$$

$$= n_G \exp(i(v_1 x)) \tag{2.9}$$

$$= n_G \exp(i(kx)) \tag{2.10}$$

where $v_1 = k$, the propagation constant or a wave number in x-direction. If a translation occurs at a length in distance, then (2.8) becomes

$$n((x+a)\vec{a}_1) = n_G \exp(i(v_1\vec{b}_1)\cdot((x+a)\vec{a}_1)) \tag{2.11}$$

$$= n_G \exp(i(v_1(x+a))) \tag{2.12}$$

$$= n_G \exp(i(v_1 x))\exp(i(v_1 a)) \tag{2.13}$$

From (2.4), $\exp(i(v_1 a)) = \exp(i2\pi) = 1$, so that

$$n((x+a)\vec{a}_1) = n_G \exp(i(v_1 x)) \tag{2.14}$$

$$= n_G \exp(i(kx)) \tag{2.15}$$

$$= n(x\vec{a}_1) \tag{2.16}$$

Thus, (2.14) becomes similar to (2.10).

Here v_1 is an integer in reciprocal lattice vector in first dimension and a is the length of the periodicity in x-direction which is assumed to be coincidence with the first dimension of the reciprocal lattice vector so that $\vec{a}_1 = \vec{a}_x$ and $v_1 = k$. Because this problem deals in the same dimension, the representation of the unit vector will be ignored.

In order to define the wave vectors, the equations above are written again in this formulation,

$$n(x) = e^{jka}n(x+a) \tag{2.17}$$

$$n(x) = n(x+a)\big|_{e^{jka}=1} \tag{2.18}$$

$$e^{jka} = 1\big|_{ka=0\,or\,2\pi} \tag{2.19}$$

$$ka = 2\pi \Leftrightarrow k = \frac{2\pi}{a} \text{ or } k = 0; \tag{2.20}$$

where (2.17) is known as the Bloch's theorem in one dimensional. From (2.19), it can be concluded that the range of k is $0 \leq k \leq 2\pi/a$ or $-\pi/a \leq k \leq \pi/a$
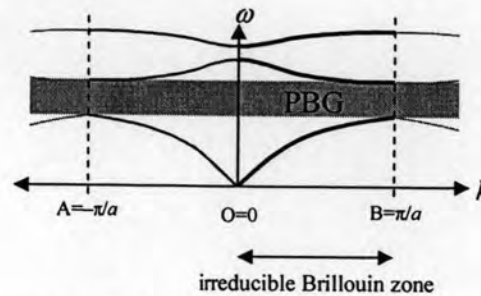

Figure 2.5 The range of the wave number in irreducible BZ of one dimensional PCs where the origin of the band gap is also shown [http://ab-initio.mit.edu]

Figure 2.5 above illustrates the range of the wave number in the irreducible BZ of one dimensional PCs. The figure shows that the origin of the band gap occurs in the symmetry edges of the first BZ at A and B.

The two dimensional case leads the Bloch's theorem in a vector form in x and y planes such that

$$n(\bar{r}) = e^{j\bar{k}.\bar{r}} n(\bar{r} + \bar{T}) \tag{2.21}$$

$$n(\bar{r}) = n(\bar{r} + \bar{T})\big|_{e^{j\bar{k}.\bar{r}}=1} \tag{2.22}$$

$$e^{j\bar{k}.\bar{r}} = 1\big|_{\bar{k}.\bar{r}=0\,or\,2\pi} \tag{2.23}$$

$$\bar{k} \cdot \bar{r} = k_x x\,\hat{a}_x + k_y y\,\hat{a}_y \tag{2.24}$$

Since the range of the wave vectors are defined in the first (square) Brillouin zone, each component of wave vectors has the same range of the values so that the ranges of k_x and k_y can be simplified as $-\frac{\pi}{a} \leq k_x, k_y \leq \frac{\pi}{a}$ which is illustrated in Figure 2.6. The ranges now is represented by the area of Γ-X-M-Γ for the square lattice and Γ-M-K-Γ for triangular lattice.
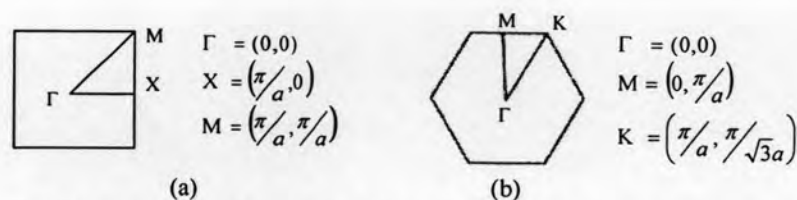

Figure 2.6 The range of the wave vectors in the irreducible BZ in (a) square and (b) triangular lattice constants.

In Figure 2.7, the wave vectors defined along the irreducible BZ for square and triangular lattices are shown to be sampled into 10 cells for each edge of the zone yielding 31 pairs of k_x and k_y. Those values are later utilized as inputs assigned in FEM formulation for nodes on the boundary of the unit cell.
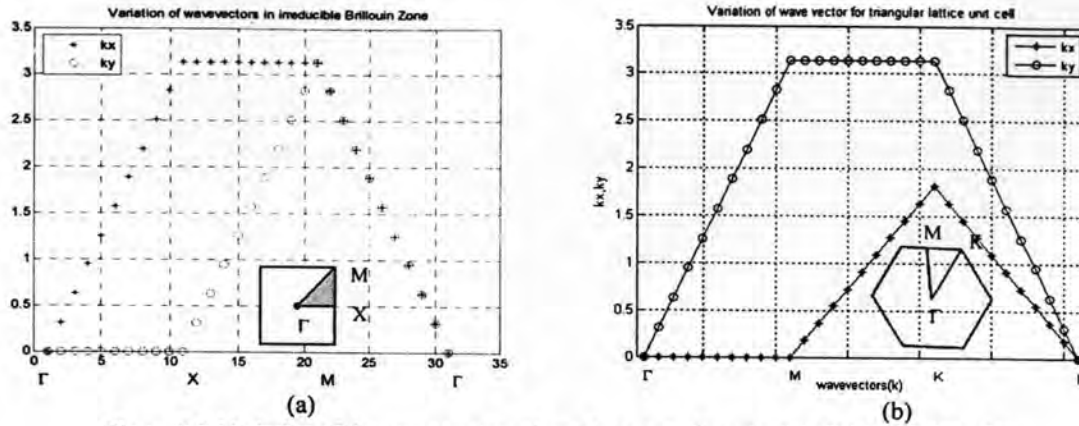

Figure 2.7 Variation of the wave vectors along the edge of irreducible Brillouin Zone for (a) square lattice and (b) triangular lattice PCs.

2.1.4 Governing equation for TM and TE waves in 2D PCs

To calculate the band gap characteristic, the famous four Maxwell's equations are basic equations. These equations are considered for an isotropic system and a non-magnetic material. Since the 2D PC is uniform along the z direction and periodicity is in the transverse plane, the consideration will be taken only for the in-plane propagation that has zero propagation constant in the z direction, $\beta_z = 0$, so that the wave modes in the PC are either TE or TM to z mode. A wave solution, in term of a Helmholtz's equation which is a two-dimensional second order derivative form, is derived from the Maxwell's equations including an application of some vector identities [12]. The wave equation is a second order derivative form of the field where the field can be an electric or a magnetic one performing a transverse electric (TE) or a transverse magnetic (TM) mode, respectively. The TE mode (E polarization) occurs when the electric field (E_{xy}) components are in-plane (x-y plane) with the periodicity and transverse or perpendicular to the propagation direction where the out-of-plane field is only the magnetic one (H_z) propagating parallel to the propagation direction (on z-axis). The same concept is applied also to the TM mode. The equations for both modes are shown as follows [3]:

TM mode:
$$-\frac{1}{\varepsilon_r}\nabla^2 E_z(x,y) = \frac{\omega^2}{c^2}E_z(x,y)$$
(2.25)

TE mode:
$$-\nabla\cdot\frac{1}{\varepsilon_r}\nabla H_z(x,y) = \frac{\omega^2}{c^2}H_z(x,y)$$
(2.26)

where ε_r is a relative permittivity of the medium of the calculation domain. The symbol ω presents an angular frequency and it is divided by the speed of light c that yields a ratio number which is an eigenvalue. This eigenvalue is a resonant frequency of the PCs

for a defined wave vector. The nabla (del) operator ∇ and the Laplacian operator ∇^2 show the derivative of a scalar field (electric field E_z and magnetic field H_z as a function of x and y) respect to x and y in first and second order form, respectively. These two equations, (2.25) and (2.26), are used in FEM formulation with periodic boundary conditions.

In previous works, the FEM formulation is taken by incorporating Bloch theorem in the governing equations of TE and TM wave subjected to periodic boundary conditions, which results in complicated FEM formulation [3,8] which are explained in sub-chapter 2.1.6. On the contrary, this work employs a straightforward FEM formulation where the Bloch function is not imposed into the governing equations but into the periodic boundary conditions. The four Maxwell's equations in derivative forms are used as the basic equations in this photonic band gap calculation. These equations are derived in source free condition, isotropic and non-magnetic medium as follows.

$$\vec{\nabla} \times \vec{E} = -\frac{\partial}{\partial t} \vec{B} = -\frac{\partial}{\partial t} \mu_o \vec{H} \tag{2.27}$$

$$\vec{\nabla} \times \vec{H} = \frac{\partial}{\partial t} \vec{D} = \frac{\partial}{\partial t} \varepsilon_0 \varepsilon_r \vec{E} \tag{2.28}$$

$$\vec{\nabla} \cdot \vec{D} = \vec{\nabla} \cdot \vec{E} = 0 \tag{2.29}$$

$$\vec{\nabla} \cdot \vec{B} = \vec{\nabla} \cdot \vec{H} = 0 \tag{2.30}$$

The first equation shows the Faraday's law and the second one is Ampere's law. These two equations are the main equations where the others two are Gauss' law that can be derived from them. $\vec{E}$ and $\vec{H}$ fields are vectors in n-dimension where the value of n depends on the interest of investigation which can be 1, 2 or 3 that corresponds to x, y and z direction in the nature. The $\vec{E}$ field consists of $\vec{E_x}, \vec{E_y}$, and $\vec{E_z}$ and so does $\vec{H}$ field. Finding the Helmholtz's equations by determining second order derivative of the $\vec{E}$ field and $\vec{H}$ field will bring us to the solution of the wave equations by transforming the forms into time harmonic solution, simply by taking an equality of $\frac{\partial}{\partial t} = -j\omega$.

There are two kinds of basic modes, transverse electric (TE) and transverse magnetic (TM) mode as shown in Figure 2.8. If the propagation axis along the waveguide is in z-direction ($\frac{\partial}{\partial z} = 0$), then TE mode occurs when all existing components of $\vec{E}$ fields are transverse (perpendicular) to the propagation axis so that, the parallel component of $\vec{E}$, $\vec{E_z}$, is equal to zero (does not exist). The same concept is taken for the TM mode. When waves propagating only along the plane of periodicity are considered, then the problems become two-dimension (2D), which is x-y plane.
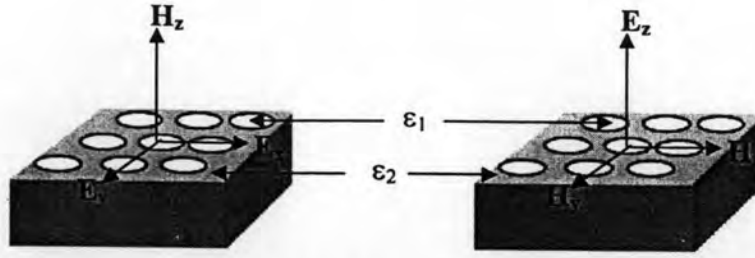
Figure 2.8 Illustration of (a) TE mode and (b) TM mode configuration on a 2D PC
with square lattice geometry.

2.1.4.1 TM modes

In TM mode, the longitudinal mode of electric fields $\overrightarrow{H_z} = 0$ while $\overrightarrow{H_x}$ and $\overrightarrow{H_y}$
exist as transverse magnetic fields and $\vec{E} = \overrightarrow{E_z} = E_z(x,y)\hat{z}$ becomes the existing
longitudinal electric fields. The wave solution for TM modes is derived by taking curl to
(2.27) and followed by substituting (2.28) so that this equation is obtained as follows,

$$\frac{1}{\varepsilon_r}\vec{\nabla} \times \vec{\nabla} \times E_z(x,y)\hat{z} = \frac{\omega^2}{c^2}E_z(x,y)\hat{z},$$
(2.31)

where ω is the (resonant) frequency of the wave, and c is the speed of light. The
parameter $\left(\dfrac{\omega^2}{c^2}\right)$ is later called eigenvalues which have to be solved numerically.

By applying the vector identity, $\nabla \times \nabla \times A = \nabla(\nabla \cdot A) - \nabla^2 A$, (2.31) becomes

$$\frac{1}{\varepsilon_r}\left(\vec{\nabla}\left(\vec{\nabla} \cdot E_z(x,y)\right) - \vec{\nabla}^2 E_z(x,y)\right) = \frac{\omega^2}{c^2}E_z(x,y)$$
(2.32)

$$\Leftrightarrow -\frac{1}{\varepsilon_r}\vec{\nabla}^2 E_z(x,y) = \frac{\omega^2}{c^2}E_z(x,y), \text{ and further becomes}$$

$$\Leftrightarrow -\frac{1}{\varepsilon_r}\left(\frac{\partial^2}{\partial x^2} + \frac{\partial^2}{\partial y^2}\right)E_z(x,y) = \frac{\omega^2}{c^2}E_z(x,y)$$
(2.33)

where ∇^2 is Laplacian operator in which $\nabla^2 A = \nabla \cdot \nabla A = \Delta A$.

2.1.4.2 TE modes

In TM mode, the longitudinal electric field $\overrightarrow{E_z} = 0$, while $\overrightarrow{E_x}$ and $\overrightarrow{E_y}$ exist as
transverse electric fields and $\vec{H} = H_z\hat{z}$ becomes the longitudinal magnetic field. The
wave solution for TM modes is derived by taking curl to (2.28) and later substituting
(2.27) so that this equation is obtained as follows,

$$\vec{\nabla} \times \frac{1}{\varepsilon_r}\vec{\nabla} \times H_z(x,y) = \frac{\omega^2}{c^2}H_z(x,y)$$
(2.34)

By applying the vector identity $\vec{a} \times (\vec{b} \times \vec{c}) = (\vec{a} \cdot \vec{c})\vec{b} - (\vec{a} \cdot \vec{b})\vec{c}$, (2.34) becomes

$$\left(\vec{\nabla} \cdot H_z(x,y)\right)\frac{1}{\varepsilon_r}\vec{\nabla} - \left(\vec{\nabla} \cdot \frac{1}{\varepsilon_r}\vec{\nabla}\right)H_z(x,y) = \frac{\omega^2}{c^2}H_z(x,y)$$

$$\Leftrightarrow -\left(\vec{\nabla} \cdot \frac{1}{\varepsilon_r}\vec{\nabla}\right)H_z(x,y) = \frac{\omega^2}{c^2}H_z(x,y)$$

$$\Leftrightarrow -\vec{\nabla} \cdot \frac{1}{\varepsilon_r}\vec{\nabla}H_z(x,y) = \frac{\omega^2}{c^2}H_z(x,y)$$

$$(2.35)$$

2.1.5 Modeling of Periodic Structures using the Bloch's Theorem
2.1.5.1 Bloch's Theorem (Floquet's Theorem)

The periodic structures can be modeled using Bloch's theorem (sometimes also called Floquet's or Bloch-Floquet's theorem). The form of the theorem is represented in Bloch wave or Bloch state[1] as follows

$$\psi_{n,\vec{k}}(\vec{r}) = e^{i\vec{k}\cdot\vec{r}}u_{n,\vec{k}}(\vec{r}) \tag{2.36}$$

A Bloch state is a wavefunction of a particle placed in a periodic potential. The state consists of a plane wave, $e^{i\vec{k}\cdot\vec{r}}$, and a periodic function (Bloch envelope), $u_{n,\vec{k}}(\vec{r})$, which has the same periodicity as the potential. The position vector $\vec{r} = (x, y, z)$. The vector $\vec{k} = (k_x, k_y, k_z)$ is the plane wave vector (Bloch wave vector) that is unique only up to a reciprocal lattice vector. Index n shows the number of calculated bands yielded from eigenfrequencies corresponding to each $\vec{k}$. A graph showing the collection of such bands and band gaps within the first Brillouin Zone (BZ) is called a band structure.

If the wave is assumed to propagate along x-direction (one-dimensional periodic structure) and to infinity, then the wave propagating in periodic structures with period a may be characterized by periodic boundary conditions or a periodically varied dielectric constant such that,

$$\psi_{n,\beta}(x) = e^{i\beta(x)}u_{n,\beta}(x) \tag{2.37}$$

$$\psi_{n,\beta}(x+a) = e^{i\beta(x+a)}u_{n,\beta}(x+a) = \psi_{n,\beta}(x) \tag{2.38}$$

Therefore, $\psi_{n,\beta}(x)$ is a periodic function of z with the period a that can be interpreted in a Fourier series,

$$\psi_{n,\beta}(x) = \sum_{n=-\infty}^{\infty} A_n e^{-i(2\pi n/a)x} \tag{2.39}$$

---

[1] The concept of the Bloch state was developed by Felix Bloch in 1928, to describe the conduction of electrons in crystalline solids. The same underlying mathematics, however, was also discovered independently several times: by George William Hill (1877), Gaston Floquet (1883), and Alexander Lyapunov (1892) [http://en.wikipedia.org/wiki/Bloch_wave].

using (2.37), (2.38) and (2.39), it is finally obtained a general expression for a wave in a periodic structure with the period a,

$$u_{n,\beta}(x) = \sum_{n=-\infty}^{\infty} A_n e^{-i(\beta+2\pi n/a)x}$$

$$= \sum_{n=-\infty}^{\infty} A_n e^{-i(\beta_n)x}, \quad \beta_n = \beta + \frac{2\pi n}{a}$$

(2.40)

The equation (2.40) shows that the wave consists of both positive-going and negative-going waves $-\infty < n < \infty$.

2.1.5.2 Imposing the Bloch's Theorem into Maxwell's Equations

Combining the two equations to model the propagating waves in the photonic crystals yields a equation form such that the fields in the Maxwell's equation is replaced by the Bloch waves (2.36) where u represents the E field or H field in a scalar form, depends on the analyzed mode. Both wave solutions, (2.32) and (2.35), then become

$$-\frac{1}{\varepsilon_r}\vec{\nabla}^2 E_z(\vec{r}) = \frac{\omega^2}{c^2}E_z(\vec{r})$$

$$\Leftrightarrow -\frac{1}{\varepsilon_r(\vec{r})}\left(\left(\vec{\nabla}_t\right)^2 e^{i\vec{k}\cdot\vec{r}}E_{zn,\vec{k}}(\vec{r})\right) = \frac{\omega_n(\vec{k})^2}{c^2}e^{i\vec{k}\cdot\vec{r}}E_{zn,\vec{k}}(\vec{r})$$

$$\Leftrightarrow -\frac{1}{\varepsilon_r(\vec{r})}\left(e^{i\vec{k}\cdot\vec{r}}\left(\vec{\nabla}_t\right)^2 E_{zn,\vec{k}}(\vec{r}) + E_{zn,\vec{k}}(\vec{r})\left(\vec{\nabla}_t\right)^2 e^{i\vec{k}\cdot\vec{r}}\right) = \frac{\omega_n(\vec{k})^2}{c^2}e^{i\vec{k}\cdot\vec{r}}E_{zn,\vec{k}}(\vec{r}) \qquad (2.41)$$

where

$$\left(\vec{\nabla}_t\right)^2 e^{i\vec{k}\cdot\vec{r}} = \left(\frac{\partial^2}{\partial x^2} + \frac{\partial^2}{\partial y^2}\right)e^{i(k_x x + k_y y + k_z z)}$$

$$= e^{i\vec{k}\cdot\vec{r}}(-k_x^2) + e^{i\vec{k}\cdot\vec{r}}(-k_y^2)$$

$$= -(k_x^2 + k_y^2)e^{i\vec{k}\cdot\vec{r}}$$

$$= -\left|\vec{k}\right|^2 e^{i\vec{k}\cdot\vec{r}} \qquad (2.42)$$

Substituting (2.42) to (2.41) yields for TM mode

$$-\frac{1}{\varepsilon_r(\bar{r})}\left(e^{i\bar{k}\cdot\bar{r}}\left(\vec{\nabla}_t\right)^2 E_{zn,\bar{k}}(\bar{r}) + E_{zn,\bar{k}}(\bar{r})\left(\vec{\nabla}_t\right)^2 e^{i\bar{k}\cdot\bar{r}}\right) = \frac{\omega_n(\bar{k})^2}{c^2}e^{i\bar{k}\cdot\bar{r}}E_{zn,\bar{k}}(\bar{r})$$

$$\Leftrightarrow -\frac{1}{\varepsilon_r(\bar{r})}\left(e^{i\bar{k}\cdot\bar{r}}\left(\vec{\nabla}_t\right)^2 E_{zn,\bar{k}}(\bar{r}) - E_{zn,\bar{k}}(\bar{r})\left|\vec{k}\right|^2 e^{i\bar{k}\cdot\bar{r}}\right) = \frac{\omega_n(\bar{k})^2}{c^2}e^{i\bar{k}\cdot\bar{r}}E_{zn,\bar{k}}(\bar{r})$$

$$\Leftrightarrow -\frac{1}{\varepsilon_r(\bar{r})}\left(\left(\vec{\nabla}_t\right)^2 - \left|\vec{k}\right|^2\right)E_{zn,\bar{k}}(\bar{r})e^{i\bar{k}\cdot\bar{r}} = \frac{\omega_n(\bar{k})^2}{c^2}e^{i\bar{k}\cdot\bar{r}}E_{zn,\bar{k}}(\bar{r})$$

$$\Leftrightarrow -\frac{1}{\varepsilon_r(\bar{r})}\left(\left(\vec{\nabla}_t\right)^2 - \left|\vec{k}\right|^2\right)E_{zn,\bar{k}}(\bar{r}) = \frac{\omega_n(\bar{k})^2}{c^2}E_{zn,\bar{k}}(\bar{r}) \tag{2.43}$$

, and for TE mode

$$-\vec{\nabla}_t \cdot \frac{1}{\varepsilon_r}\vec{\nabla}_t H_z = \frac{\omega^2}{c^2}H_z$$

$$\Leftrightarrow -\vec{\nabla}_t \cdot \frac{1}{\varepsilon_r(\bar{r})}\left(\vec{\nabla}_t e^{i\bar{k}\cdot\bar{r}}H_{zn,\bar{k}}(\bar{r})\right)$$

$$\Leftrightarrow -\vec{\nabla}_t \cdot \frac{1}{\varepsilon_r(\bar{r})}\left(H_{zn,\bar{k}}(\bar{r})\vec{\nabla}_t e^{i\bar{k}\cdot\bar{r}} + e^{i\bar{k}\cdot\bar{r}}\vec{\nabla}_t H_{zn,\bar{k}}(\bar{r})\right)$$

$$\Leftrightarrow -\vec{\nabla}_t \cdot \frac{1}{\varepsilon_r(\bar{r})}\left(H_{zn,\bar{k}}(\bar{r})\left(ik_x\hat{x} + ik_y\hat{y}\right)e^{i\bar{k}\cdot\bar{r}} + e^{i\bar{k}\cdot\bar{r}}\vec{\nabla}_t H_{zn,\bar{k}}(\bar{r})\right)$$

$$\Leftrightarrow -\vec{\nabla}_t \cdot \frac{1}{\varepsilon_r(\bar{r})}\left(\left(\vec{\nabla}_t + \left(ik_x\vec{x} + ik_y\vec{y}\right)\right)e^{i\bar{k}\cdot\bar{r}}H_{zn,\bar{k}}(\bar{r})\right)$$

$$\Leftrightarrow -\left(\frac{\partial}{\partial x}\hat{x} + \frac{\partial}{\partial y}\hat{y}\right)\cdot\frac{1}{\varepsilon_r(\bar{r})}\left(\left(\left(\frac{\partial}{\partial x} + ik_x\right)\hat{x} + \left(\frac{\partial}{\partial y} + ik_y\right)\hat{y}\right)e^{i\bar{k}\cdot\bar{r}}H_{zn,\bar{k}}(\bar{r})\right)$$

$$\Leftrightarrow -\vec{\nabla}_t \cdot \frac{1}{\varepsilon_r(\bar{r})}\left(\left(\vec{\nabla}_t + i\vec{k}\right)e^{i\bar{k}\cdot\bar{r}}H_{zn,\bar{k}}(\bar{r})\right)$$

$$\Leftrightarrow -\left(\vec{\nabla}_t + i\vec{k}\right)\cdot\frac{1}{\varepsilon_r(\bar{r})}\left(\vec{\nabla}_t + i\vec{k}\right)H_{zn,\bar{k}}(\bar{r}) = \frac{\omega_n(\bar{k})^2}{c^2}H_{zn,\bar{k}}(\bar{r}) \tag{2.44}$$

2.1.6 Comparison of the governing equations with the previous FEM works

Previous works done by W. Axmann and P. Kuchment (1999) and B.P. Hiett, et.al. (2002) employed the Bloch function into the governing equation in order to model the periodicity of the structure as in (2.43) and (2.44) and used them as the FEM formulation which becomes more complicated compared to the formulation proposed in this work. Table 2.1 shows the difference between those formulations.

Table 2.1 Comparison of formulations used in the previous and recent works

Type of mode	Previous work	Recent work
TE mode	$-\left(\vec{\nabla}_t + i\vec{k}\right)\cdot\dfrac{1}{\varepsilon_r(r)}\left(\vec{\nabla}_t + i\vec{k}\right)H_{zn,\bar{k}}(\bar{r}) = \dfrac{\omega_n(\bar{k})^2}{c^2}H_{zn,\bar{k}}(\bar{r})$	$-\vec{\nabla}\cdot\dfrac{1}{\varepsilon_r}\vec{\nabla}H_z(x,y) = \dfrac{\omega^2}{c^2}H_z(x,y)$
TM mode	$-\dfrac{1}{\varepsilon_r(r)}\left(\left(\vec{\nabla}_t\right)^2 - \left|\vec{k}\right|^2\right)E_{zn,\bar{k}}(\bar{r}) = \dfrac{\omega_n(\bar{k})^2}{c^2}E_{zn,\bar{k}}(\bar{r})$	$-\dfrac{1}{\varepsilon_r}\vec{\nabla}^2 E_z(x,y) = \dfrac{\omega^2}{c^2}E_z(x,y)$

From the table above, it can be seen that the recent formulations are straightforward taken from Helmholtz's equations. The only parameter included in the formulation evaluation is the relative permittivity, ε_r, while those fields are unknowns and the ratio between the angular frequency and the speed of light is the eigenvalue of the eigensystem formulation.

2.2 Domain discretization over a unit cell

According to the FEM, the calculation domain must be discretizised in order to get the approximation solution. The discretization or meshing yields finite number of elements where unknown parameters are assign at nodes in the mesh. The typical element can be triangular or rectangular shape.
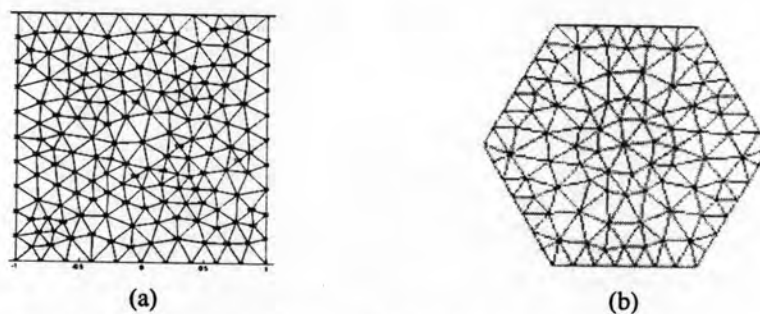

(a)   (b)

Figure 2.9 Discretizised (a) square and (b) triangular lattice unit cell shows the matched position of nodes on the parallel boundary to provide the condition for PBC

Figure 2.9 shows the discretizised domains with triangular elements for both types of unit cells. A typical triangular element with local node numbering is shown in Figure 2.10.
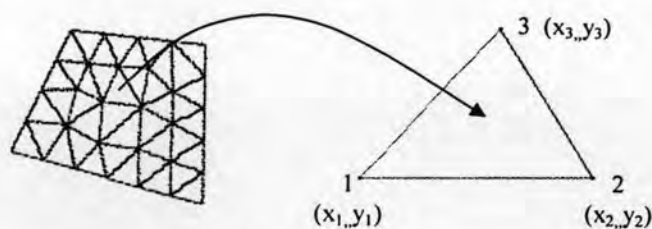

Figure 2.10 Typical triangular finite element mesh using a linear element type

A linear (3-node) triangular element is the simple type of triangle, also known as a first order element as shown in Figure 2.10. The higher order element gives the higher accuracy with the more complicated interpolation function. The chosen type of element depends on the order of polynomial function using in the interpolation function. The interpolation function is known as a basis function or a shape function. The detail of shape function will be explain more in section 2.3.

The important consideration in meshing on this unit cell is that the linear discretization in a pair of parallel boundary lines must yield the same number of nodes which are also parallel to each other where the periodic boundary conditions (PBC) will be imposed on them in order to model the periodicity of the structure. This consideration must be taken in meshing with polygonal elements as well which brings the problem into the polygonal FEM discussed in Chapter 3.

2.3   Selecting the interpolation function N_i^e

The next step is finding the interpolation function or the shape function, N_i^e, used to provide the approximation of the unknown solution within each element [15]. The polynomial expression that is employed as interpolation function can be linear (first order) or non-linear (high order). The higher order polynomial will give the higher accuracy in the solution. The important feature of this function is that the function N_i^e must be nonzero only within element e and must be vanished outside element e. The properties of the shape function are defined as follows [16, 18]:

1. Form a partition of unity to assure constant precision, and that $N_i^e(\bar{x})$ is non-negative and bounded:

$$\sum_{i=1}^{n} N_i^e(\bar{x}) = 1, \quad 0 \le N_i^e(\bar{x}) \le 1$$

2. Interpolate nodal data where the first property ensures that the interpolated result is bounded between the minimum and maximum of the nodal values as stated as $\min_i \phi_i^e \le \bar{\phi}^e(\bar{x}) \le \max_i \phi_i^e$. This statement tells about the discrete maximum principle and a requirement for the numerical discretization of the diffusion equation.

3. Execute linear completeness or linear precision,

$$\sum_{i=1}^{n} N_i^e(\bar{x})\bar{x}_i = \bar{x}$$

    This property indicates that the shape functions can exactly reproduce a linear function. In second-order partial differential equations (PDEs), constant and linear precision in the trial function are sufficient conditions for convergence in a Galerkin method.

4. Present the shape function $N_i^e(\bar{x})$ as an element of C^∞ within the domain. Along the edges of the polygon, the interpolant must be piece-wise linear (C^0 function):

$$\bar{\phi}(t) = t\bar{\phi}_1 + (1-t)\bar{\phi}_2; \quad \bar{x} = t\bar{x}_1 + (1-t)\bar{x}_2; \quad \bar{x} \in \partial\Omega, t \in [0, 1].$$

The above equation ensures that linear essential boundary conditions can be imposed exactly in a Galerkin method including the periodic boundary conditions.

This research will compare the performance of FEM using the interpolation function that is obtained from triangular and polygonal elements, shown in Figure 1.3. The main difference between triangular FEM and polygonal FEM is how to construct the shape function. This function is built based on the type of elements used as the sub-domains where it is influenced by the number of the vertices constructing the element, the surface area of the element, and the chosen order of the interpolation system. This shape function is later used to approximate the unknown in the element. The order of the function depends on the usage of mid points and side points on the edge of the boundary and also the interior points inside the element.

The triangular elements are so flexible that have been used for the past 30 years because they can model any arbitrary geometries. Triangulation completely partitions the domain into smaller triangular elements. The shape function of triangular elements is normally determined by using area coordinates and Lagrange interpolation polynomials. In the type of linear triangulation, the shape function is expressed in term of area coordinates or barycentric[2] coordinates for triangular elements [12].

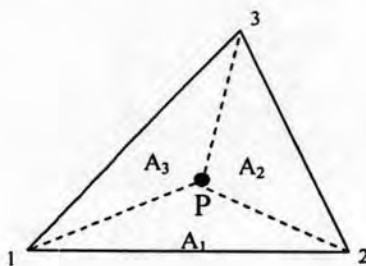### 2.3.1 Area coordinates concepts

Figure 2.11 Area coordinate concept on a triangular element

A typical application of area coordinates is to interpolate any data (not just positions) provided at the vertices of P [19]. An area coordinate formulated in (2.47) is a ratio between the area of a partially smaller triangle (constructed by a point $P(x,y)$ inside the element and two vertices of local nodes on the outer boundary of the original triangular element) and the area of the original triangular element shown in Figure 2.11.

The areas of the smaller triangles in one triangle element are given by [12]

$$A_1^e = A^e(p,1,2) = \frac{1}{2}\begin{vmatrix} x & y & 1 \\ x_1 & y_1 & 1 \\ x_2 & y_2 & 1 \end{vmatrix}, \quad A_2^e = A^e(p,2,3) = \frac{1}{2}\begin{vmatrix} x & y & 1 \\ x_2 & y_2 & 1 \\ x_3 & y_3 & 1 \end{vmatrix} \text{ and } A_3^e = A^e(p,3,1) = \frac{1}{2}\begin{vmatrix} x & y & 1 \\ x_3 & y_3 & 1 \\ x_1 & y_1 & 1 \end{vmatrix} \quad (2.45)$$

---

[2] Barycentric means satisfying the linear precision property

The area of the element will give a positive number if the vertices are numbered counterclockwise which is written as follows:

$$A^e = A^e(1,2,3) = \frac{1}{2}\begin{vmatrix} x_1 & y_1 & 1 \\ x_2 & y_2 & 1 \\ x_3 & y_3 & 1 \end{vmatrix} \tag{2.46}$$

The area coordinates L_i^e for $i = 1, 2$ and 3 in element e is given as follows:

$$L_i^e = \frac{Ai^e}{A^e} \Rightarrow L_i^e(x,y) = \frac{Ai^e(x,y)}{A^e} \tag{2.47}$$

2.3.2 Linear/first-order interpolation function

As mentioned before, the area coordinate is used as the interpolation function so that $N_i^e = L_i^e$. Inside the linear triangular element constructed by 3 nodes and 3 linear edges, the unknown ϕ is approximated and is symbolized as $\overline{\phi}^e$. The approximation is taken using an expansion with the interpolation function as shown in (2.48) as described in the first and the third properties of the shape function.

$$\overline{\phi}^e = \sum_{i=1}^{3} L_i^e \phi_i^e \text{ while } 1 = \sum_{i=1}^{3} L_i^e \tag{2.48}$$

In linear triangular elements, the interpolation function is the area coordinates where $N_i^e = L_i^e$ such that the shape functions become:

$$N_1^e(x,y) = \frac{[(x_1 y_2 - x_2 y_1) + (y_1 - y_2)x + (x_2 - x_1)y]^e}{2A^e}, \tag{2.49}$$

$$N_2^e(x,y) = \frac{[(x_2 y_3 - x_3 y_2) + (y_2 - y_3)x + (x_3 - x_2)y]^e}{2A^e} \tag{2.50}$$

$$N_3^e(x,y) = \frac{[(x_3 y_1 - x_1 y_3) + (y_3 - y_1)x + (x_1 - x_3)y]^e}{2A^e}, \tag{2.51}$$

in which $N_i^e(x_j, y_j) = \begin{cases} 1, & i = j \\ 0, & i \neq j \end{cases}$ illustrated in Figure 2.12.

In order to increase the accuracy of the approximate solution which means to reduce the error related to the exact solutions or semi-analytical solutions, there are two kinds of method, one of which is increasing the order of elements while the other one is increasing the number of elements on the same calculation domain. The last method can be obtained by refining mesh so that more number of unknowns from more elements will be evaluated while keeping the order of elements, which means that the order of the interpolation function is not changed. However, changing the order of elements will

modify the design of nodes in each element by adding more nodes. The interpolation function must be changed as well so that the approximate solution based on the nodal unknowns can be obtained more accurately. For example, a second order element, which is also called as a quadratic element, will utilize a quadratic polynomial interpolation function assigned for six nodes on each element.
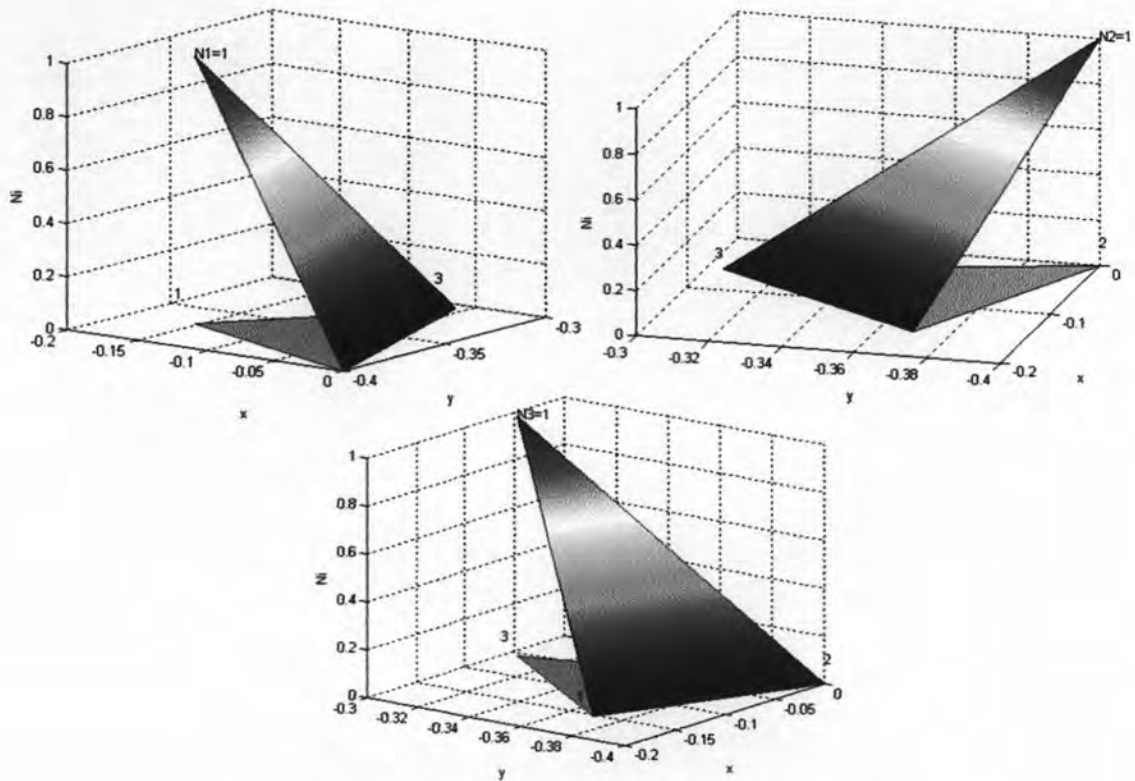

Figure 2.12 Shape functions on a linear triangular element

2.4   Formulation of the equation system
2.4.1   Galerkin's methods

After the discretization, the weak equation of the wave solution for each mode is solved by FEM imposing the PBC using the Galerkin's method. First, the governing equation for this two-dimension scalar FEM equation is taken from a wave solution of Helmholtz's equation. Here, the general equation is shown for the wave solution for both TE and TM mode in (2.25) and (2.26) [12, 15]

$$\nabla \cdot [p(x,y)\nabla \phi(x,y)] + \left(\frac{\omega}{c}\right)^2 q(x,y)\phi(x,y) = f(x,y) \tag{2.52}$$

If there is no source forced to the system, then $f(x,y)=0$. When it is applied to TE mode (or H_z polarization),

$$\phi(x,y) = H_z(x,y), \qquad p(x,y) = \frac{1}{\varepsilon_r}, \qquad q(x,y) = \mu_r \tag{2.53}$$

while for TM mode (E_z polarization),

$$\phi(x,y) = E_z(x,y), \quad p(x,y) = \frac{1}{\mu_r}, \quad q(x,y) = \varepsilon_r \tag{2.54}$$

where the relative permeability $\mu_r=1$ for non-magnetic material.

If the TM mode solution is taken into consideration first, then the wave equation in (2.54) is derived as follows:

$$\nabla \cdot [\nabla E_z(x,y)] + \left(\frac{\omega}{c}\right)^2 \varepsilon_r E_z(x,y) = 0 \tag{2.55}$$

$$\Leftrightarrow \nabla^2 E_z(x,y) + \left(\frac{\omega}{c}\right)^2 \varepsilon_r E_z(x,y) = 0 \tag{2.56}$$

If the approximate $\underline{E_z}$ field is represented as $\bar{\phi}(x,y)$, then the above equations become a residual function or an error function represented as r below

$$r = \nabla \cdot [\nabla\bar{\phi}(x,y)] + \left(\frac{\omega}{c}\right)^2 \varepsilon_r \bar{\phi}(x,y) \tag{2.57}$$

$$= \nabla^2\bar{\phi}(x,y) + \left(\frac{\omega}{c}\right)^2 \varepsilon_r \bar{\phi}(x,y) = 0 \tag{2.58}$$

For simplifying the form, $\bar{\phi}(x,y)$ is written as $\bar{\phi}$ only from now and finally (2.58) becomes

$$r = \frac{\partial^2\bar{\phi}}{\partial x^2} + \frac{\partial^2\bar{\phi}}{\partial y^2} + \left(\frac{\omega}{c}\right)^2 \varepsilon_r\bar{\phi} \tag{2.59}$$

By multiplying equation (2.59) with a weighting function w which is a function of x and y and by integrating over all the domain of calculation, the weighted residual function R is obtained as in (2.60) which is forced to be zero following the concept of Galerkin method so that R is represented as follows:

$$R = \int_\Omega wr dxdy = 0 \tag{2.60}$$

$$= \int_\Omega w\left(\frac{\partial^2\bar{\phi}}{\partial x^2} + \frac{\partial^2\bar{\phi}}{\partial y^2} + \left(\frac{\omega}{c}\right)^2 \varepsilon_r\bar{\phi}\right) dxdy$$

$$= \iint w\frac{\partial^2\bar{\phi}}{\partial x^2} dxdy + \iint w\frac{\partial^2\bar{\phi}}{\partial y^2} dxdy + \iint w\left(\frac{\omega}{c}\right)^2 \varepsilon_r\bar{\phi} dxdy$$

$$= \int\left[\int w\frac{\partial^2\bar{\phi}}{\partial x^2} dx\right]dy + \int\left[\int w\frac{\partial^2\bar{\phi}}{\partial y^2} dy\right]dx + \iint w\left(\frac{\omega}{c}\right)^2 \varepsilon_r\bar{\phi} dxdy$$

$$= \int\left[\int wd\left(\frac{\partial\bar{\phi}}{\partial x}\right)\right]dy + \int\left[\int w\left(\frac{\partial\bar{\phi}}{\partial y}\right)\right]dx + \iint w\left(\frac{\omega}{c}\right)^2 \varepsilon_r\bar{\phi} dxdy$$

$$= \int\left[w\frac{\partial\bar{\phi}}{\partial x} - \int\frac{\partial\bar{\phi}}{\partial x}\frac{\partial w}{\partial x} dx\right]dy + \int\left[w\frac{\partial\bar{\phi}}{\partial y} - \int\frac{\partial\bar{\phi}}{\partial y}\frac{\partial w}{\partial y} dy\right]dx + \iint w\left(\frac{\omega}{c}\right)^2 \varepsilon_r\bar{\phi} dxdy$$

$$= \int w \frac{\partial \bar{\phi}}{\partial x} dy + \int w \frac{\partial \bar{\phi}}{\partial y} dx - \iint \left(\frac{\partial \bar{\phi}}{\partial x} \frac{\partial w}{\partial x} + \frac{\partial \bar{\phi}}{\partial y} \frac{\partial w}{\partial y} \right) dx dy + \iint w \left(\frac{\omega}{c} \right)^2 \varepsilon_r \bar{\phi} dx dy$$

$$= \int w \left(\frac{\partial \bar{\phi}}{\partial x} dy + \frac{\partial \bar{\phi}}{\partial y} dx \right) - \iint \left(\frac{\partial \bar{\phi}}{\partial x} \frac{\partial w}{\partial x} + \frac{\partial \bar{\phi}}{\partial y} \frac{\partial w}{\partial y} \right) dx dy + \iint w \left(\frac{\omega}{c} \right)^2 \varepsilon_r \bar{\phi} dx dy$$

$$= \int w \frac{\partial \bar{\phi}}{\partial n} d\Gamma - \iint \left(\frac{\partial \bar{\phi}}{\partial x} \frac{\partial w}{\partial x} + \frac{\partial \bar{\phi}}{\partial y} \frac{\partial w}{\partial y} \right) dx dy + \iint w \left(\frac{\omega}{c} \right)^2 \varepsilon_r \bar{\phi} dx dy \qquad (2.61)$$

The weighting function in Galerkin's method is not imposed to the unknowns on the boundary (in the line integration part) but it is imposed on each element or the sub-domain so that the line integration part can be omitted from the weighted residual function R since boundary nodes will be assigned for the boundary conditions. Finally, (2.61) becomes

$$R = -\iint \left(\frac{\partial \bar{\phi}}{\partial x} \frac{\partial w}{\partial x} + \frac{\partial \bar{\phi}}{\partial y} \frac{\partial w}{\partial y} \right) dx dy + \iint w \left(\frac{\omega}{c} \right)^2 \varepsilon_r \bar{\phi} dx dy \quad \text{where } \bar{\phi} = \sum_{i=1}^{n} N_i^e \phi_i^e \qquad (2.62)$$

In (2.14), it is shown that the unknown ϕ in one element is approximated by an expansion of multiplication between the unknown value on each vertex i (ϕ_i^e) with its shape function or also called a basis function N_i^e which is a function of x and y. Forcing $R=0$, an eigensystem (2.63) is obtained by the expression below taken from (2.62)

$$-\iint \left(\frac{\partial \left(\sum_{i=1}^{n} N_i^e \phi_i^e \right)}{\partial x} \frac{\partial w}{\partial x} + \frac{\partial \left(\sum_{i=1}^{n} N_i^e \phi_i^e \right)}{\partial y} \frac{\partial w}{\partial y} \right) dx dy + \iint w \left(\frac{\omega}{c} \right)^2 \varepsilon_r \left(\sum_{i=1}^{n} N_i^e \phi_i^e \right) dx dy = 0$$

$$\Leftrightarrow \iint \left(\frac{\partial [N_i^e]^T \{\phi^e\}}{\partial x} \frac{\partial w}{\partial x} + \frac{\partial [N_i^e]^T \{\phi^e\}}{\partial y} \frac{\partial w}{\partial y} \right) dx dy = \iint w \left(\frac{\omega}{c} \right)^2 [N_i^e]^T \{\phi^e\} \varepsilon_r dx dy \qquad (2.63)$$

The expression in (2.63) yields the weak formulation of the system. In Galerkin's method, the weighting function w as a function of the space (x and y) is the same as the used shape function so that the approximation becomes optimized. Finally, the (2.63) can be expressed as follows.

$$\iint \left(\frac{\partial [N_i^e]}{\partial x} \frac{\partial [N_i^e]^T}{\partial x} \{\phi^e\} + \frac{\partial [N_i^e]}{\partial y} \frac{\partial [N_i^e]^T}{\partial y} \{\phi^e\} \right) dx dy = \left(\frac{\omega}{c} \right)^2 \iint [N_i^e][N_i^e]^T \{\phi^e\} \varepsilon_r dx dy \qquad (2.64)$$

$$\Leftrightarrow \left[\iint \left(\frac{\partial [N_i^e]}{\partial x} \frac{\partial [N_i^e]^T}{\partial x} + \frac{\partial [N_i^e]}{\partial y} \frac{\partial [N_i^e]^T}{\partial y} \right) dx dy \right] \{\phi^e\} = \left(\frac{\omega}{c} \right)^2 \left[\iint [N_i^e][N_i^e]^T \varepsilon_r dx dy \right] \{\phi^e\} \qquad (2.65)$$

$$\Leftrightarrow [A^e]\{\phi^e\} = \left(\frac{\omega}{c} \right)^2 [B^e]\{\phi^e\} \qquad (2.66)$$

$$\Leftrightarrow [A]\{\phi\} = \lambda[B]\{\phi\} \qquad (2.67)$$

where

$$[A] = \sum_e [A^e], \quad [B] = \sum_e [B^e], \quad \text{and} \quad \{\phi\} = \sum_e \{\phi^e\}.$$

The expression in (2.66) states the eigensystem over elements of element matrices which later are mapped into a global matrix as in (2.67) with λ represents the eigenvalues. The mapping from element matrices to the global matrix is run using a relation $K^e_{pq} = K_{t(p,e),t(q,e)}$ where p and q are the row and the column number of the matrix K^e, respectively.

From (2.65), the main functions used in the programming code of the FEM formulation is related to the shape functions N_i^e for $i = 1,2,3$ as in (2.49)-(2.51) while the others are constants. Converting the shape functions and their derivatives into programming language can be learnt more in [12] that gives more clearance about the programming construction for numerical method for such linear triangular FEM.

2.4.2   Assigning the periodic boundary conditions (PBC)

From master equation in (2.61), there is a part consisting of the line integration for the unknown on the outside boundary. For these unknown nodes on the boundary, the periodic boundary condition (PBC) will be imposed. In FEM, boundary conditions must be applied to the system in order to get the approximate solutions. Since PCs are periodic, imposing periodic boundary conditions (PBC) to the nodes on the outer edges of the calculation domain on the mirroring sides is suitable for an efficient calculation. FEM divides the original domain into smaller areas (sub-domains) and creates a discretizised domain.

PBC require that the domain discretization must contemplate that on each pair of mirroring edges, the number of nodes must be equal and those nodes on each edge must be parallel to nodes on its pair edge in order to keep the periodicity of the structures [3, 11]. The PDETOOL in MATLAB, GiD v.8, and Plaxis are some examples of mesh generation softwares that aid to discretizise over the calculation domain as shown in Figure 2.13. By designing the mesh carefully using the mesh generator, the parallelism of sub-division in mirroring edges can be obtained for both square and triangular lattice PCs.
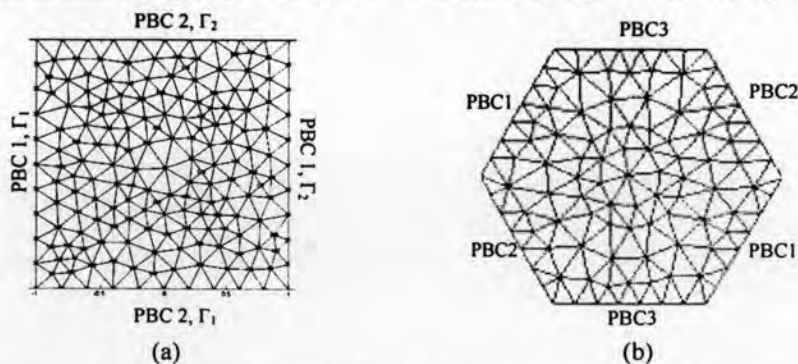

Figure 2.13 Discretizised (a) square and (b) triangular lattice unit cell shows the matched position of nodes on the parallel boundary to provide the condition for PBC

Figure 2.13 shows a sample of square domain where the PBC can be imposed on. The length of the periodicity is presented as a unit length that is related to the absolute value of two-dimension vector in x-y plane. The PBC are imposed to nodes on the boundary of the domain.

For the square unit cell, the PBC can be expressed as in [7]

PBC 1: $\qquad \phi(x+a,y)\big|_{\Gamma_2} = e^{-jk_x a}\phi(x,y)\big|_{\Gamma_1}$ $\qquad\qquad\qquad$ (2.68)

PBC 2: $\qquad \phi(x,y+a)\big|_{\Gamma_2} = e^{-jk_y a}\phi(x,y)\big|_{\Gamma_1}$ $\qquad\qquad\qquad$ (2.69)

while for the triangular unit cell, the expressions for the PBC are

PBC 1: $\qquad \phi\left(x+\dfrac{\sqrt{3}a}{2}, y-\dfrac{a}{2}\right)\Big|_{\Gamma_2} = e^{-j\left(k_x\sqrt{3}a/2 - k_y a/2\right)}\phi(x,y)\big|_{\Gamma_1}$ $\qquad$ (2.70)

PBC 2: $\qquad \phi\left(x+\dfrac{\sqrt{3}a}{2}, y+\dfrac{a}{2}\right)\Big|_{\Gamma_2} = e^{-j\left(k_x\sqrt{3}a/2 + k_y a/2\right)}\phi(x,y)\big|_{\Gamma_1}$ $\qquad$ (2.71)

PBC 3: $\qquad \phi(x,y+a)\big|_{\Gamma_2} = e^{-jk_y a}\phi(x,y)\big|_{\Gamma_1}$ $\qquad\qquad\qquad$ (2.12)

where Γ_1 and Γ_2 are a pair of parallel edges where independent nodes and dependent nodes exist, respectively.

The PBC in (2.68) and (2.69) are applied for each pair of mirroring nodes thus the position of the nodes on the boundary is very important as shown in Figure 2.14 where node 1, 7 and 9 are dependent to node 3 while node 4 and 8 are dependent to node 6 and 2, respectively. Imposing PBC will modify the element matrices which are assembled to form the generalized eigenvalues problem which is solved as a function of k. For each k, the solver computes a set of eigenvalues. These eigenvalues are plotted as a function of k to give a dispersion relation or a band gap characteristic. The union of band functions for all k represents the density of states for the modes of the original problem. It gives a clear visual indication of any band gaps as the density drops to zero for those frequency ranges.
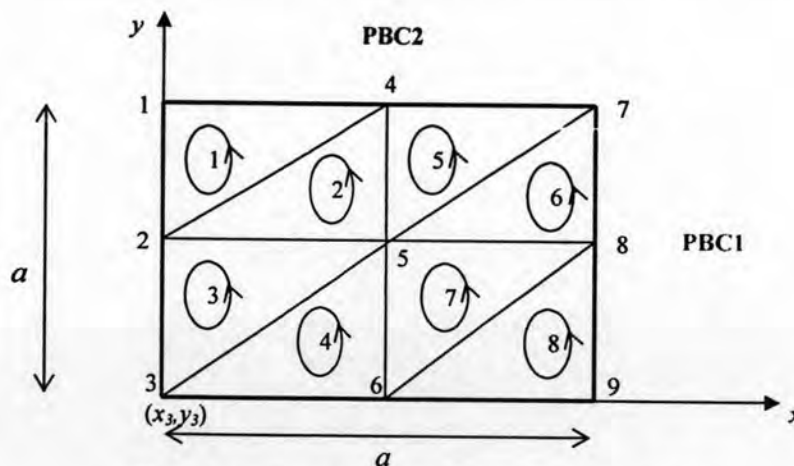

Figure 2.14 Sample calculation domain imposing PBC

Applying the PBC will modify the generated matrices in the eigensystems since the nodes imposed by PBC on the mirroring edges, such as node 1,4,7,8, and 9 shown in Figure 2.14, will be removed from the calculation. It is done due to the redundancy with their pairing nodes, such as node 2,3, and 6. In this case, the sizes of the eigen-matrices are reduced related to the number of redundant nodes lying on the mirroring edges.

2.5 Summary of the FEM process

As a summary, the whole processes of the FEM are illustrated in a flowchart shown in Figure 2.15. The process marked with a star is the part where another shape function can be applied in FEM that leads the polygonal FEM instead of linear triangular FEM.
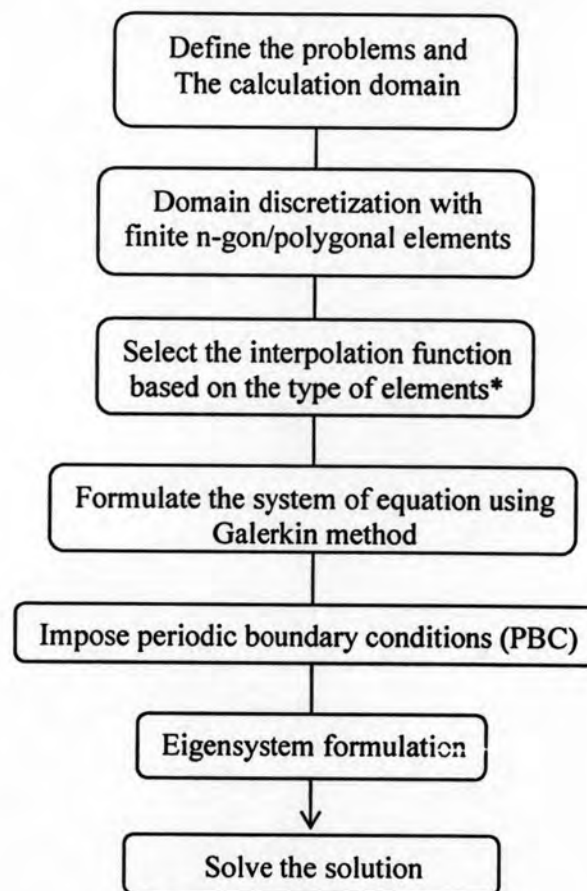
Define the problems and
The calculation domain

Domain discretization with
finite n-gon/polygonal elements

Select the interpolation function
based on the type of elements*

Formulate the system of equation using
Galerkin method

Impose periodic boundary conditions (PBC)

Eigensystem formulation

Solve the solution

Figure 2.15 FEM process